5-23-2019

Impact of oxygen plasma treatment on carrier transport and molecular adsorption in graphene

Hongmei Li
Clemson University, hongmel@g.clemson.edu

Austin Singh
University of Central Florida

Ferhat Bayram
Clemson University

Anthony S. Childress
Clemson University

Apparao Rao
Clemson University, arao@clemson.edu

See next page for additional authors

ARTICLE

Impact of oxygen plasma treatment on carrier transport and molecular adsorption in graphene

Hongmei Li,*[a] Austin Singh,[a,c] Ferhat Bayram,[a] Anthony S. Childress,[b] Apparao M Rao[b] and Goutam Koley[a]

Received 00th January 20xx,
Accepted 00th January 20xx

DOI: 10.1039/x0xx00000x

Impact of plasma treatment on graphene's transport properties and interaction with gas molecules has been investigated with Raman, X-ray photoelectron spectroscopy, and Hall measurements. Experimental results indicate the formation of nanocrystalline domains and enhanced fraction of adsorbed oxygen following oxygen plasma treatment, which correlates with a significant reduction in carrier mobility and an increase in carrier density. The oxygen plasma treated graphene was found to exhibit much stronger sensitivity toward NH_3 molecules both in terms of magnitude and response rate, attributable to increased domain edges and oxygen adsorption related enhancement in p-type doping. The carrier mobility in plasma exposed graphene was modeled considering both ionized impurity and short-range scatterings, which matched well with experimentally observed mobility.

Introduction

Graphene's unique material properties, especially its two-dimensional nature, a combination of strong σ- and weaker π-bonds, as well as low electrical noise, have led to a strong interest in exploring its sensing ability in the past decade. Its high surface-to-volume ratio and unsaturated π-bonds facilitate interaction with molecular and ionic adsorbates, leading to the investigation of a large variety of sensors for many different applications including chemical and biomolecular detection, ionic detection, as well as infrared and radiation detection.[1-5] In spite of its widely observed interaction with molecules leading to their physisorption or chemisorption, it is believed that such pristine, not-defective graphene is not very interactive with molecules, and cannot be used to develop highly sensitive sensors.[6] In other words, the defects in graphene contribute to its observed strong interaction with molecules. Indeed, the sensitivity of graphene to analyte molecules is often enhanced with surface functionalization, which may themselves lead to defects in the graphene layer given its atomically thin nature. Using either a solvent assisted process, or sputtered metal oxide or nanoparticle decoration on the graphene's surface, researchers have attempted to modify graphene's electrical properties, and, as such, it's sensing characteristics.[6-8] However, the surface functionalization methods are generally associated with various issues including agglomeration of graphene layers, bad uniformity for large area dispersion, and processing complexity.[9] Alternatively, plasma treatment of graphene, which also generates defects, can be a simple, clean, and very effective alternative approach to functionalizing the graphene surface, with the goal of enhancing its sensitivity. Although there are existing reports addressing the chemical and physical effect of plasma treatment on graphene, studies on the direct impact of plasma treatment on the enhancement of molecular interaction capability of graphene and its sensing ability have not been reported yet.

In this article, we conducted a systematic study on the effect of defect introduction in graphene through O_2 plasma treatment, utilizing Raman spectroscopy, Hall measurements, and XPS analysis. A carefully controlled O_2 plasma exposure of graphene led to significant changes in transport property and a strong improvement in the rate and extent of interaction with NH_3 molecules. An empirical model proposed to estimate carrier mobility in plasma treated graphene showed very good agreement with experimental results.

Experimental

The graphene used in this study was synthesized on copper foil (Alfa Aesar, 99.999%) using a home-built CVD system. Ultra-high purity CH_4, H_2 and Ar gases were used in the ratio of 1:1:9 during graphene growth at 1035 °C for 20 min. The graphene was then transferred onto a SiO_2/Si substrate using a wet transfer process.[7] PMMA was spin-coated on graphene to work as the sacrificial layer, while ammonium persulfate solution was used to etch the copper away and release the graphene/PMMA layer. The graphene/PMMA double layer was then transferred onto the SiO_2/Si substrate and PMMA was removed through acetone treatment. For Hall measurements, Ti/Ni metal stacks were deposited at the four corners of 6 × 6 mm graphene on SiO_2

[a] Department of Electrical and Computer Engineering, Clemson University, South Carolina, 29825, USA.
[b] Department of Physics and Astronomy, Clemson University, South Carolina, 29825, USA
[c] College of Optics & Photonics, University of Central Florida, Orlando, Florida, 32816, USA

Electronic Supplementary Information (ESI) available: [details of any supplementary information available should be included here]. See DOI: 10.1039/x0xx00000x

substrate using a shadow mask. Hall measurements were conducted using a commercial set up HMS 3000 (Ecopia, Inc.) retrofitted with gas flow tubes and mass flow controllers. This system allows Hall measurements to be conducted in desired gaseous environments. Further details about setup can be found in an earlier report.[10] To study the effect of plasma treatment on the molecular interaction property of graphene, it was exposed to 475 ppm NH_3 gas diluted in N_2 sequentially after various durations of plasma treatment. The oxygen plasma was generated with a plasma etch system PE25-JW (Plasma Etch, Inc.) with a starting pressure of 200 mTorr before flowing oxygen gas. The graphene was plasma treated for 2 – 14 s at a power of 37.5 W, with a constant 15 sccm oxygen flow. To determine the quality of post-exposure graphene, Raman spectra were obtained with 532 nm excitation wavelength (InVia, Renishaw plc.) before and after various durations of O_2 plasma treatment and compared. Also, X-ray photoelectron spectroscopy (XPS) (VersaProbe III, Physical Electronics, Inc.) was used to investigate the graphene's surface chemical composition variation caused by the plasma treatment.

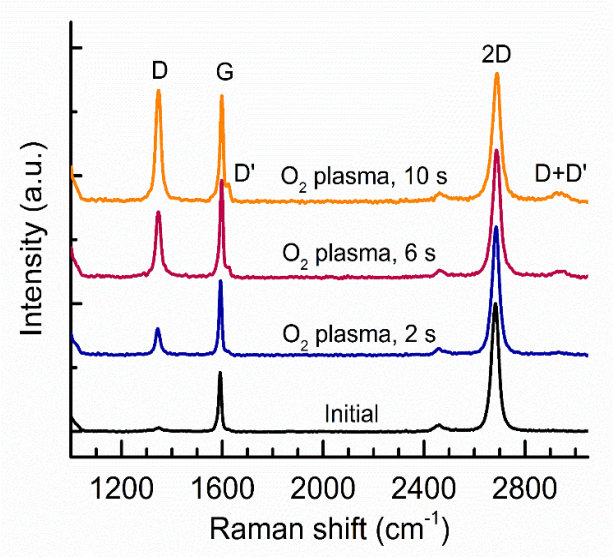

FIG. 1. Raman spectra of initial graphene (bottom), and O_2 plasma treated graphene for durations of 2 s, 6 s, 10 s, are compared. The observed reduction of 2D/G peak intensity ratio and increase in the magnitude of the D peak is by O_2 plasma treatment induced disorder in graphene's atomic structure.

Results and discussion

Figure 1 compares the Raman spectra of the initial untreated graphene with O_2 plasma treated graphene with exposure durations of 2, 6, and 10 seconds. The three main peaks of graphene, i.e. D, G and 2D can be found in each spectrum. The initial graphene exhibits intensity ratios of $I_{2D}/I_G \approx 2.2$ and $I_D/I_G \approx 0.06$, which indicates that its monolayer nature and high quality is preserved even after transfer to the SiO_2/Si substrate. [11] When exposed to low power O_2 plasma (carefully avoiding over damage), a gradual change in Raman spectroscopic characteristics is observed as a function of exposure time. We find that the I_{2D}/I_G is reduced monotonically from initial 2.2 to 1.7, 1.3, and finally to 1.2; while the I_D/I_G values increased from 0.06 to 0.35, 0.68, and 1.05 corresponding to the exposure durations of 2, 6, 10 s, respectively. Even though $I_{2D}/I_G \approx 1$ is widely accepted as an indication of double layer graphene, in this case it is caused by suppression of the lattice vibration mode induced by defects on single layer graphene.[12] Along with disordered sp^2-bond induced high rising of D peak, two other peaks D' (~1620 cm^{-1}) and D+D' (~2940 cm^{-1}) can also be observed after 6s plasma exposure, which is consistent with previous observations.[12] From the increasing disorder peaks, we can conclude that even though with very low plasma exposure power and duration, it induced significant damage to the graphene's atomic structure. The domain size in defective graphene, which is an important parameter determining short range scattering, can be calculated from the intensity ratio I_D/I_G. Using the relationship $I_D/I_G = C'(\lambda)/L_d^2$, proposed by Lucchese et al. [13] and utilizing the Tuinstra-Koenig relation (where $C'(\lambda)$ is given as 102 nm^2 for 514 nm laser excitation), we estimate the defective graphene's nanocrystalline domain size, L_d, of 49.0, 17.0, 12.3, 9.8 µm for 0, 2, 6, 10 s plasma treatment, respectively. The value of L_d after 4s of H_2 plasma treatment was determined to be 5.4 µm from the I_D/I_G value of 3.5 obtained from the Raman spectrum included in supplemental Fig. S1.

To further investigate the effect of O_2 plasma treatment on the graphene's interaction with gaseous molecules, its response to 475 ppm NH_3 exposure was recorded using the Hall measurement system, which simultaneously yields conductivity (σ), carrier density (n_s) and mobility (μ_{Hall}). NH_3 gas was flown over the sample and alternately switched on and off for 10 mins duration, to record the changes in electrical characteristics and recovery. The values of conductivity, carrier density, and mobility measured after every few minutes using the Hall system are plotted in Fig. 2. We find that graphene's carrier (hole) density drops with the NH_3 exposure, which is expected since NH_3 is a typical electron donor for graphene.[10, 14-15] Interestingly, mobility increases with NH_3 adsorption on graphene, which is consistent with our earlier study. [10] When NH_3 molecules interact with graphene, they lose electrons and become positively charged impurities. Typically, ionized impurities on graphene's surface affect its carrier transport properties by inducing carrier scattering which can cause a reduction in mobility. However, in this case instead of decreasing mobility, the positively charged NH_3 ions screen the scattering effects of the negatively charged ionized impurities present initially on graphene (commonly observed in graphene transferred on SiO_2 [16]). This screening process, and consequent increase in mobility, has been explained in detail in our previous report. [10] The conductivity, which is proportional to the product of carrier density and mobility, follows the same trend as carrier density, which shows a proportionally higher change compared to mobility. Comparing the responses corresponding to the various duration of plasma treatment, we find that the changes in conductivity, carrier density, and mobility increased initially, reached the highest level (55%, 76%,

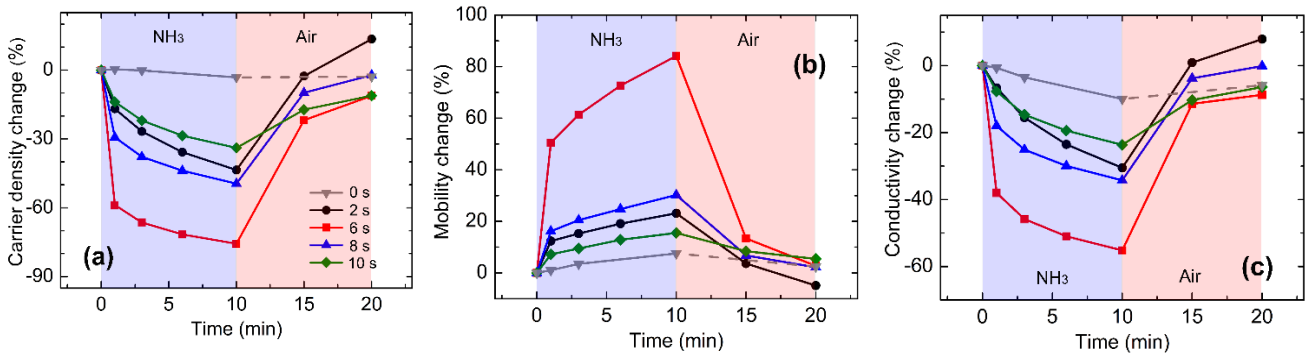

FIG. 2. O_2 plasma treated graphene's response to 475 ppm NH_3 gas in terms of (a) carrier density, (b) mobility, and (c) conductivity, for 0 – 10 s of plasma exposure. Maximum response is observed for 6 s exposure for all three parameters. Dotted grey line indicate expected recovery transient estimated from longer duration measurements.

and 84%, respectively) for the 6s plasma treated graphene, and then kept reducing for 8 and 10 s exposure durations. We can see that the response rate for 6s plasma treated graphene is the fastest, with more than half of the maximum response occurring within the first minute, while the response magnitudes (for all three parameters) are also comparatively much higher. The transients for initial graphene is also shown for reference (recovery transient estimated from longer duration measurements, which is discussed below).

Although the 6s exposure led to the best response, and exposing graphene for more or less time to O_2 plasma led to a reduced response to NH_3, those are still better than the untreated graphene's response. Indeed, comparing the initial untreated graphene's and plasma treated (6 s) graphene's responses to NH_3 gas (shown Fig. 3 with moderate sensing performance for each sample), we find that O_2 plasma treated graphene's sensing performance improved dramatically both in response magnitude (increased over 750 % over the first 10 min exposure) and response rate (reduced 40 times considering the initial 20 % change). H_2 plasma treatment also showed some

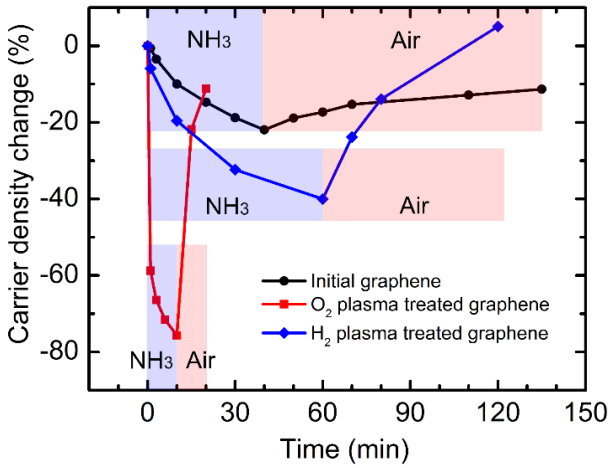

FIG. 3. Comparison of the response (percentage carrier density change measured by Hall system) toward 475 ppm NH_3 between untreated graphene, 6 s O_2 plasma and 2 s H_2 plasma treated graphene. Both the magnitude and rate of response are very significantly enhanced after O_2 plasma treatment, while only a minor improvement is noticed after H_2 plasma treatment.

enhancement effect on graphene's NH_3 sensing as shown in Fig. 3, the details will be discussed further in a following section.

Figure 4 shows the variation in graphene's electrical properties due to O_2 plasma treatment as a function of treatment time. We find that the carrier density increases monotonically while conductivity and mobility decrease as the treatment time is increased from 0 to 14 s. From the Raman spectroscopy results discussed above, a reduction in mobility is expected, due to increased scattering effect from increased disorder and nano-crystalline domains formed in graphene due to plasma treatment. On the other hand, the increased carrier density can be attributed to an increase in oxygen adsorption on the graphene surface following plasma treatment, as reported in earlier studies.[12,17,18] Keeping in mind the very low power and plasma exposure time, XPS studies were carried out to confirm if indeed such an increase in oxygen bonding on the graphene surface occurred. In addition, since exposure to H_2 plasma is expected to act in an opposite way to O_2 plasma exposure, we also performed electrical and XPS characterization on H_2 plasma treated graphene samples, and the XPS spectra and carrier transport characteristics were compared between initially untreated, O_2 plasma treated, and H_2 plasma treated graphene.

Table 1 summarizes the effects of O_2 and H_2 plasma treatment (at 37.5 W power level for a duration of 10 s and 4 s,

TABLE I. Change in carrier mobility and density and conductivity of graphene following 4 s O_2 and H_2 plasma treatments.

Graphene Parameter		μ ($cm^2V^{-1}s^{-1}$)	n_s ($10^{12}/cm^2$)	σ ($\Omega^{-1}cm^{-1}$)
H_2 plasma treatment	Before	1.7×10^3	2.9	1.6×10^3
	After	7.3×10^1	1.8	4.1×10^1
O_2 plasma treatment	Before	1.7×10^3	3.0	1.7×10^3
	After	2.8×10^2	12.5	1.1×10^3

respectively) on the conductivity, mobility, and density of the

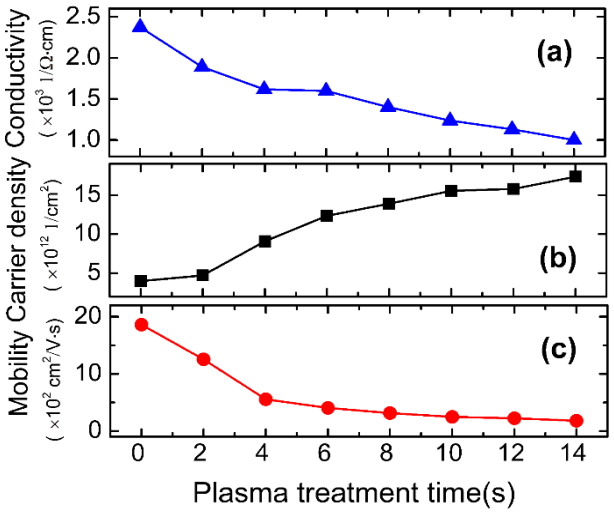

FIG. 4. Variation in (a) conductivity, (b) sheet carrier density, (c) carrier mobility in graphene as a function of O_2 plasma treatment time. We find the carrier (hole) density increases, while the mobility and conductivity (proportional to the product of mobility and carrier density) decreases monotonically with exposure time.

carriers in graphene. We find from Table 1 that both O_2 and H_2 plasma treatment reduces carrier mobility in graphene. In contrast, however, the H_2 plasma exposure reduces carrier density by ~39% in graphene, while O_2 plasma exposure increases it by ~310%. As discussed above, the mobility reduction can be attributed to an increase in disorder and nano-crystalline domains formed in graphene, as revealed through Raman spectroscopy, and is expected to result, in general, from plasma exposure irrespective of the gaseous species (and corresponding ions) involved. On the other hand, a reduced carrier density by H_2 plasma treatment (unlike an increase in case of O_2 plasma treatment) can be explained considering the formation of C-H bonds or removal of oxygen bonds through reacting with pre-adsorbed oxygen on the graphene surface, both of which can result in an n-doping effect. [19, 20]

The validity of the proposed mechanisms for change in carrier density due to an increase or decrease in adsorbed oxygen (due to O_2 and H_2 plasma treatments, respectively) was tested through XPS spectroscopic studies. For this, a graphene sample (on SiO_2 substrate) was split into two pieces, with one subjected to O_2 plasma and the other to H_2 plasma treatment. C1s XPS spectra of initial graphene, O_2 plasma treated graphene, and H_2 plasma treated graphene were taken and are shown in Fig. 5. The spectra are fitted to Gaussian curve peaks of sp^2 bonds, sp^3 hybridization, as well as, C-OH, and O-C=O at binding energies of ~284.6, ~285.6, 286.6 and 288.8 eV, respectively. The ratios of area under the respective Gaussian curve (for C-OH and O-C=O curves) were calculated and the percentages are shown in the figure, from which we find that the O_2 plasma treatment caused an increase in the ratio of adsorbed oxygen (15.5 + 13.0 = 28.5%) in graphene while H_2 plasma treatment reduced it (12.7 + 10.4 = 23.1%), compared to the initial untreated graphene (14.2 + 10.1 = 24.3%). These results clearly indicate that even with very low power and short duration of plasma exposure, both O_2 and H_2 plasma could significantly affect the ratio of pre-adsorbed oxygen on the graphene surface, causing the observed change in carrier density as discussed above. The relative magnitude of changes in carrier density (which are in opposite directions), following O_2 and H_2 plasma treatments (Table 1), also correlate well with the changes in the ratio of oxygen in graphene following the plasma treatments. We also note that a similar approach for inducing p-doping graphene, through the formation of carbon-oxygen bonds (C-O or C=O), by activation of O_2 with UV light, has been reported recently. [20]

As discussed earlier, plasma treated graphene exhibit a significant enhancement in its interaction with NH_3 molecules. The Raman and XPS studies indicate that after plasma treatment the graphene crystalline structure gets significantly altered, as well as the ratio of absorbed oxygen on graphene increases. The enhancement in interaction with NH_3, and related enhancement in sensing property can be attributed to two major factors: structural damage and consequent enhancement in adsorbed oxygen caused by plasma treatment, and change in Fermi level due to enhanced p-type doping. From earlier reports, the domain edges of graphene (offering so-called "dangling bonds") created by plasma treatment can provide a large number of additional vacant sites for NH_3 molecules to attach, and the ensuing higher charge transfer can strongly change the conductivity as well as sensitivity. [21] In addition, an increase in bonded oxygen species on graphene (see earlier discussion on XPS results) also play a significant role

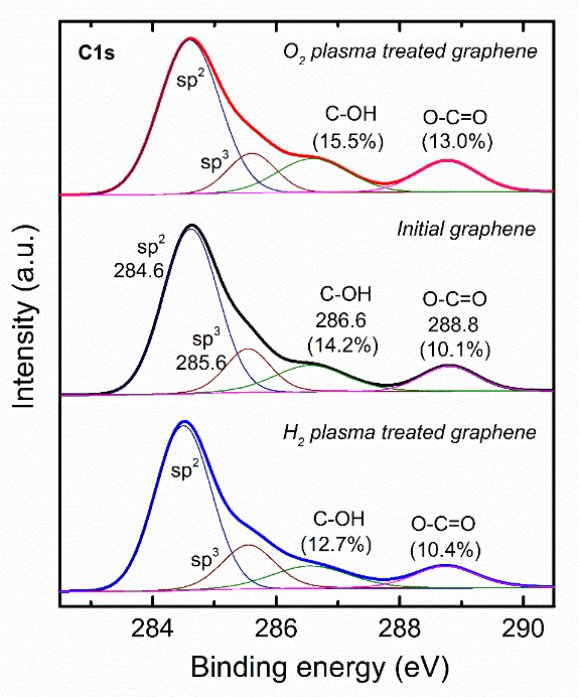

FIG. 5. Comparison of the C1s XPS spectra of untreated graphene (black, center panel), O_2 plasma treated graphene (red, top panel), and H_2 plasma treated graphene (blue, bottom panel). The fraction of area of the curves showing adsorbed oxygen in graphene (C-OH and O-C=O bonds) can be seen to be significantly higher after O_2 plasma treatment, but lower after H_2 plasma treatment.

in enhancing graphene's sensitivity to NH_3. *Lee et al.* reported density functional theory (DFT) calculations on graphene in which they found a much lower NH_3 adsorption energy (E_{ads}) at bonded oxygen species (-0.16 ~ 0.25 eV) sites compared to the vacancy sites (-1.48 eV) in graphene (see the referred paper for schematic structures of adsorption).[21] A lower E_{ads} indicates a faster and easier adsorption process for the NH_3 molecules. Thus, the oxygen plasma treated graphene facilitates adsorption of NH_3 molecules on its surface, and when coupled with water vapor (from ambient as well as at the graphene/SiO_2 interface due to wet processing) they subsequently interact with graphene and transfer charges. [22] Indeed for H_2 plasma treated graphene, which led to a decrease in adsorbed oxygen (see above discussion) the carrier concentration was reduced leading to only slightly higher sensing performance (20% change in 10 min, 32% change in 30 min; refer to Fig. 3) compared to that of the pristine graphene (10% change in 10 min, 19% change in 30 min). Here the effect of the increase in domain edge dangling bonds contributed to enhanced sensitivity, but the reduction in adsorbed oxygen (from H_2 plasma treatment) did not offer any additional enhancement in sensitivity (unlike O_2 plasma treatment), and may even have reduced it to some extent.

The second factor causing sensitivity improvement can be related to the downward movement of the Fermi level in graphene due to enhanced p-type carrier density (Fig. 4). In earlier research, Singh et al. reported that the graphene's sensitivity to NH_3 can be enhanced by increasing the p-type doping in it by application of a negative gate voltage in a back-gated transistor configuration. [23] This is because the energy gap between the defect state induced by adsorbed NH_3 and the Fermi level in graphene increases as the latter one moves down due to high p-type doping. Since the carrier density in the graphene increases significantly after O_2 plasma treatment, the Fermi level also moves lower significantly, increasing the gap with NH_3 donor states, and hence enhancing sensitivity. Following the similar argument, NO_2, which is a well-known acceptor molecule in graphene, shown having its sensitivity affected only minimally after oxygen plasma treatment, as the energy gap between the acceptor state induced by NO_2 reduces as the graphene becomes more p-type, which reduces the charge transfer between those states.[23] This was indeed observed experimentally, where graphene's sensitivity to NO_2 molecules did not show noticeable improvement as to NH_3 with oxygen plasma treatment.

Although ionized impurity (Coulomb) scattering has been proposed as the dominant mechanism limiting carrier mobility in graphene. [24 – 26], however, since plasma treated graphene has significant structural defects, short-range scattering can also be expected to strongly affect its carrier mobility. Indeed mobility was found to decreases sharply, after plasma exposure, regardless of whether the carrier density increased or decreased (Table 1). This contradicts commonly observed increase in mobility with a reduction in carrier density and vice versa, generally observed when ionized impurity scattering is predominant. [10, 26] Clearly, for plasma treated graphene, both short-range and Coulomb scattering should be considered as important factors affecting carrier mobility. Following Matthiessen's rule, the overall mobility can be expressed as

$$\frac{1}{\mu_{gr\_pls}} = \frac{1}{\mu_{imp}} + \frac{1}{\mu_{sr}}, \qquad (1)$$

where μ_{gr_pls} is the overall carrier mobility in graphene (after plasma treatment), μ_{imp} is the carrier mobility limited by ionized impurity scattering, and μ_{sr} is the carrier mobility limited by short-range scattering. From the analytical model proposed by *Shaffique Adam et al*. (2007) mobility in graphene, with high charged impurity concentration, is inversely proportional to impurity concentration. [27] Therefore, μ_{imp} can be described as

$$\mu_{imp} = \mu_{init} \times K \frac{n_{init}}{n_{gr\_pls}}, \qquad (2)$$

where μ_{init}, n_{init} are graphene's initial carrier mobility (1860 $cm^2/V{\cdot}s$) and carrier concentration (3.98×10^{12} cm^{-2}) (shown in Table S2), and n_{gr_pls} is the carrier concentration after plasma treatment, and K is the proportionality constant. On the other hand, considering the relationship between graphene's crystal domain (L_d) and defect density (n_d) following plasma exposure, $L_d = n_d^{-1/2}$ [13], and the linear relationship between defect density n_d and carrier density n [28], one can write $L_d \propto n^{-1/2}$ or $L_d \propto (1/\mu^{-1/2})$ taking into account the inversely proportional relationship between mobility and impurity concentration. [27] The short-range scattering limited mobility μ_{sc} can then be expressed as

$$\mu_{sr} = \mu_{init} \times M \left(\frac{L_d}{L_{d\_init}}\right)^2, \qquad (3)$$

where M as a proportionality constant. Using the set of measured transport data from a graphene (after the sample was sequentially exposed to O_2 plasma in 2 s increments until 14 s), the calculated values of L_d discussed earlier (Table S1), the proportionality constants K and M in equations 2 and 3 were determined iteratively as 1.5 and 9.1, respectively, minimizing the standard deviation between the measured and modeled mobility (least square fit). Figure 6 shows the fit between

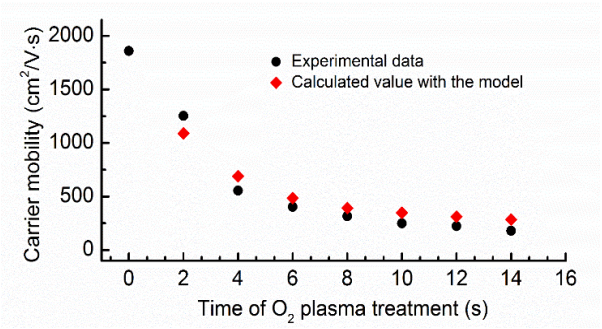

FIG. 6. Variation in the experimentally measured and calculated mobility as a function of O_2 plasma treatment time, indicating a very good match between the experimental and modeled mobility.

measured and modeled carrier mobility using equations 1 – 3. The calculated values can be seen to be in very good agreement with the measured data for all the plasma exposure times. We would like to point out here that when the scattering mechanisms are considered individually, the fit with the experimental data is not as good. The fit between the modeled mobility, considering only ionized impurity or short range scattering, and the experimental data, are shown in Fig. S2 for different values of K and M. The ionized impurity scattering model agrees better on the higher mobility side (Fig. S2 (a)), while the short-range scattering model fits better for lower mobility side (Fig. S2 (b)), where stronger crystal structure's distortion can induce short-range scattering. This clearly underlines the need for considering both ionized impurity and short-range scattering in modeling the carrier transport in defective graphene.

Conclusions

In conclusion, we have demonstrated a strong influence of oxygen plasma treatment on carrier transport properties of graphene and its ability to interact with gaseous molecules such as NH_3. Raman spectroscopic measurements indicate the formation of smaller nanocrystalline domains with increasing duration of plasma exposure of graphene, while, XPS measurements indicate an enhancement in the fraction of adsorbed oxygen. Hall measurements demonstrate a carrier mobility reduction following plasma treatment that is attributable to enhanced short-range scattering, and an increase in carrier density resulting from a higher fraction of adsorbed oxygen in graphene. The magnitude and response rate for NH_3 molecule sensing, increased dramatically with plasma exposure, with a peak enhancement recorded after 6 s of exposure. The carrier mobility in plasma treated graphene was modeled considering both ionized impurity and short-range scattering, which agreed very well with the experimentally measured mobility.

Conflicts of interest

There are no conflicts to declare.

Acknowledgements

Financial support for this work from the National Science Foundation (Grants Nos. CBET-1606882, IIP-1602006, and EEC-1560070) is thankfully acknowledged.

1 T. Kuila, S. Bose, P. Khanra, A. K. Mishra, N. H. Kim and J. H. Lee, *Biosens. Bioelectron*., 2011, **26(12)**, 4637.
2 E. Singh, M. Meyyappan and H. S. Nalwa, *ACS Appl. Mater. Interfaces*, 2017, **9(40)**, 34544.
3 H. Li, Y. Zhu, M. S. Islam, M. A. Rahman, K. B. Walsh and G. Koley, *Sens. Actuators, B*, 2017, **253**, 759.
4 I. J. Luxmoore, P. Q. Liu, P. Li, J. Faist and G. R. Nash, *ACS photonics*, 2016, **3(6)**, 936.
5 E. Cazalas, B. K. Sarker, I, Childres, Y. P. Chen and I Jovanovic, *Appl. Phys. Lett*. 2016, **109(25)**, 253501.
6 W. Fu, C. Nef, O. Knopfmacher, A. Tarasov, M. Weiss, M. Calame and C. Schönenberger, *Nano Lett.,* 2011, **11(9)**, 3597.
7 M. A. Uddin, A. K. Singh, T. S. Sudarshan and G. Koley, *Nanotechnol*., 2014, **25(12)**, 125501.
8 X. Wang, S. M. Tabakman and H. Dai, J. Am. *Chem. Soc*., 2008, 130**(26)**, 8152.
9 T. Kuila, S. Bose, A. K. Mishra, P. Khanra, N. H. Kim and J. H. Lee, *Prog. Mater Sci*., 2012, **57(7)**, 1061.
10 H. Li, X. Han, A. S. Childress, A. M. Rao and G. Koley, *Physica E,* 2019, **107**, 96.
11 L. M. Malard, M. A. Pimenta, G. Dresselhaus and M. S. Dresselhaus, *Phys. Rep*., 2009, **473(5-6)**, 51.
12 I. Childres, L. A. Jauregui, J. Tian and Y. P. Chen, *New J. Phys*., 2011, **13(2)**, 025008.
13 M. M. Lucchese, F. Stavale, E. M. Ferreira, C. Vilani, M. V. O. Moutinho, R. B. Capaz, C. A. Achete and A. Jorio, *Carbon*, 2010, **48(5)**, 1592.
14 B. K. Daas, G. Koley and T. S. Sudarshan, *Sensors & Transducers*, 2017, **216(9/10)**, 29.
15 M. A. Uddin, A. Singh, K. Daniels, T. Vogt, M. V. S. Chandrashekhar and G. Koley, *Jpn. J. Appl. Phys.,* 2016, **55(11)**, 110312.
16 M. Ishigami, J. H. Chen, W. G. Cullen, M. S. Fuhrer and E. D. Williams, *Nano Lett.,* 2007, **7(6)**, 1643.
17 A. Nourbakhsh, M. Cantoro, T. Vosch, G. Pourtois, F. Clemente, M. H. van der Veen, J. Hofkens, M. M. Heyns, S. De Gendt and B. F. Sels, *Nanotechnol.*, 2010, **21(43)**, 435203.
18 W. Choi, H. Nishiyama, Y. Ogawa, Y. Ueno, K. Furukawa, T. Takeuchi, Y. Tsutsui, T. Sakurai and S. Seki, *Adv. Opt. Mater*., 2018, **6(14)**, 1701402.
19 A. Goto, G. Takeuchi, R. Yamachi, T. Tanaka, T. Takahashi and K. Uchida, *ECS Trans*., 2016, **72**, 7.
20 M. Z. Iqbal, A. Rehman and S. Siddique, *Appl. Surf. Sci*., 2018, **451**, 40.
21 G. Lee, G. Yang, A. Cho, J. W. Han and J. Kim, *Phys. Chem. Chem. Phys*., 2016, **18(21)**, 14198.
22 Z. Zhang, X. Zhang, W. Luo, H. Yang, Y. He, Y. Liu, X Zhang and G. Peng, *Nanoscale Res. Lett*., 2015, **10(1)**, 359.
23 A. K. Singh, M. A. Uddin, J. T. Tolson, H. Maire-Afeli, N. Sbrockey, G. S. Tompa, M. G. Spencer, T. Vogt, T. S. Sudarshan and G. Koley, *Appl. Phys. Lett*., 2013, **102(4)**, 043101 .
24 C. Lombardi, S, Manzini, A, Saporito and M. Vanzi, *IEEE Trans. Comput. Aided Des. Integr. Circuits Syst*., 1988, **7(11)**,1164.
25 E. H. Hwang, S. Adam and S. D. Sarma, *Phys. Rev. Lett*., 2007, **98(18)**, 186806.
26 S. Adam, E. H. Hwang and S. D. Sarma, *Physica E*, 2008, 40**(5)**, 1022.
27 S. Adam, E. H. Hwang, V. M. Galitski and S. D. Sarma, A self-consistent theory for graphene transport. *Proceedings of the National Academy of Sciences*, 2007, **104(47)**, 18392.
28 L. Zhao, R. He, K. T. Rim, T. Schiros, K. S. Kim, H. Zhou, C. Gutiérrez, S. P. Chockalingam, C. J. Arguello, L. Pálová and D. Nordlund, *Science*, 2011, **333(6045)**, 999.

